UCRL-CONF-204448

LAWRENCE
LIVERMORE
NATIONAL
LABORATORY

Simulation of Plasma Fluxes to Material Surfaces with Self-consistent Edge Turbulence and Transport for Tokamaks

T.D. Rognlien, M.V. Umanksy, X.Q. Xu, R.H. Cohen, L.L. LoDestro

June 2, 2004

16th Plasma Surface Interaction Conference
Portland, ME, United States
May 24, 2004 through May 28, 2004

Disclaimer

UCRL-CONF-204448

Simulation of plasma fluxes to material surfaces with self-consistent edge turbulence and transport for tokamaks

T.D. Rognlien, M.V. Umansky, X.Q. Xu,
R.H. Cohen, and L.L. LoDestro

*University of California Lawrence Livermore National Laboratory,
Livermore, California 94551 USA*

Abstract

The edge-plasma profiles and fluxes to the divertor and walls of a divertor tokamak with a magnetic X-point are simulated by coupling a 2D transport code (UEDGE) and a 3D turbulence code (BOUT). An relaxed iterative coupling scheme is used where each code is run on its characteristic time scale, resulting in a statistical steady state. Plasma variables of density, parallel velocity, and separate ion and electron temperatures are included, together with a fluid neutral model for recycling neutrals at material surfaces. Results for the DIII-D tokamak parameters show that the turbulence is preferentially excited in the outer radial region of the edge where magnetic curvature is destabilizing and that substantial plasma particle flux is transported to the main chamber walls. These results are qualitatively consistent with some experimental observations. The coupled transport/turbulence simulation technique provides a strategy to understanding edge-plasma physics in more detailed than previously available and to significantly enhance the realism of predictions of the performance of future devices

1 Introduction

The distribution of plasma fluxes to material surfaces is a key issue for fusion devices because it identifies peak heat loads, and determines hydrogenic and impurity particle sources via recycling and sputtering. The wall fluxes can erode the material, setting its lifetime, and inject undesirable impurities into the plasma discharge. The typical modeling approach for tokamaks has been to simulate the scrape-off layer (SOL) plasma with 2D transport codes that assume enhanced turbulence-induced transport across the magnetic field to fit experimental profiles. Plasma turbulence simulations for fixed profiles, *e.g.*, Ref. [1], show that turbulent fluxes of the required magnitude arise from instabilities driven by radial plasma gradients. However, because the profiles and turbulence are strongly coupled, being able to predict the plasma fluxes in future devices such as ITER requires coupling of simulations for turbulence and profile evolution. The approach reported here is coupling the BOUT 3D turbulence code [1] with the UEDGE 2D transport code [2]. Initial coupling of only the plasma density variable for fixed temperature profiles is presented in rogn04. For the present paper, the coupling is extended to the electron and ion temperatures and the parallel velocity. Neutrals are treated self-consistently via a flux-limited fluid model with parallel inertia.

One feature of our simulations is a strong outward convection of the plasma in the far scrape-off layer. Such behavior has been observed or inferred by various diagnostics, such as Langmuir probes, Gas-Puff imaging, and imaging of background H_α light ([3,4] and references therein). Analysis of polarization of plasma density "blobs" from opposite ion and electron ∇B drifts, and the resulting $\mathbf{E} \times \mathbf{B}$ drift, appear to explain the rapid outward motion [5]. The impact of large SOL edge-plasma transport has been analyzed previously by the empirical approach of fitting transport coefficients to those deduced from experimental data [6–8].

The approach taken in this paper is to determine the transport by coupling with a 3D turbulence simulation that includes both closed and open B-field line regions near the magnetic separatrix. The combined model thus yields the size and generation rate of the "blobs" from plasma turbulence, and includes the cross-B-field transport and particle recycling. Because the characteristic time scales of the turbulence is short and the profile evolution time scale can be long (owing to recycling), an iterative scheme [9] is used that relaxes the turbulent fluxes passed from BOUT to UEDGE and the profiles from UEDGE to BOUT over many coupling steps. Each code is run on its own characteristic time scale, yielding a statistically averaged steady state. An limited version of this coupling for the edge plasmas is reported in Ref. [10]. Since the turbulent fluxes are coupled directly to UEDGE with no assumption of small-amplitude diffusive transport, and the effects of convective transport events are included. Because the turbulence code is relatively time consuming compared to the transport code, a substantial savings in time can be realized compared to a straightforward running of the turbulence code on transport time scales.

The paper presents the simulation models and coupling procedure in Sec. 2 and gives results applied to DIII-D in Sec. 3. A discussion and summary are provided in Sec. 4.

2 Transport and turbulence models and coupling

The physics model for the edge plasma is taken from the strongly magnetized fluid equations of Braginskii [11] with some reductions as described in Refs. [1,2]. The 2D UEDGE and 3D BOUT codes use a common poloidal-radial mesh as shown in Fig. 1, which is based on magnetic flux surfaces, and turbulence code includes segment of the toroidal dimension. UEDGE evolves the primary toroidally averaged variables denoted by uppercase letters; namely, plasma and neutral densities ($N_{i,n}$), parallel ion and velocities ($V_{\|i,n}$), and electron and ion temperatures ($T_{e,i}$). Here the electrostatic potential (Φ) comes from the inertialess parallel electron momentum equation.

BOUT evolves fluctuating quantities with zero toroidal average, and these are denoted as lower-case variables. For the electrostatic limit used in this paper, there are six fluctuating field quantities: n_i, $v_{\|i}$, $v_{\|e}$, ϕ, t_e, and t_i, where electron momentum and vorticity equations are included. The turbulence has various drive mechanisms, including the destabilizing combination of magnetic curvature and decaying density on the outside of the torus, and the negative sheath resistance of the divertor plate sheath [1]. It is assumed that neutrals do not have a direct impact on the plasma turbulence. For the present case, we suppress the turbulence in the private flux region. Characteristics of the edge turbulence are discussed in a separate paper at this conference [12].

The transport equations are the form of a convection-diffusion system with source terms. The equations thus have the form

$$\frac{\partial \Psi_k}{\partial t} + \nabla \cdot (\mathbf{V}_k \Psi_k - D_k \nabla \Psi_k) = S_k, \tag{1}$$

where Ψ_k denote different plasma and neutral variables given above. The source/sink represent processes like ionization, recombination, energy loss, and also pressure work terms for the energy equations [2]. Standard edge-plasma boundary conditions are applied, where here we fix the plasma variables at the core boundary. Particle recycling occurs at the divertor plates and outer wall, and energy transmission coefficients are used at these surfaces.

As illustrated in Ref. [10], there can be a large separation in the time scale of the turbulence growth and saturation (denoted $\tau_1 \sim 10^{-4}$ s) on the one hand and the profile evolution (denoted $\tau_2 \sim 10^{-2}$ s) on the other. This separation lends itself to an iterative coupling between the transport and turbulence as an efficient way to obtain consistent profiles and turbulence. To implement the approach, we perform toroidal and temporal averages of the BOUT radial fluxes, $\Gamma_{rk} = \langle \psi_k v_r \rangle$. Here the turbulent radial velocity is determined by the fluctuating $\mathbf{E}\times\mathbf{B}$ velocity, $v_r = -\nabla_2 \phi / B$, where ∇_2 denotes the derivative in the direction normal to B and the magnetic flux surface (radial). These fluxes are then used to define V_{rk} and D_{rk} within UEDGE to yield a consistent flux, *i.e.*

$$\Gamma_{rk} = V_{rk}\Psi_k - D_{rk}\nabla_r\Psi_k \tag{2}$$

As long as the fluxes match, it does not matter for the transport how the flux is divided between convection (V_{rk}) and diffusion (D_{rk}). Inclusion of the convective term allows one to including fluxes that may move "up" the gradient of Ψ_k, and diffusion tends to be more robust numerically. For the energy equations, the "source terms" also involve nonlinear averages of turbulent quantities [*e.g.*, $v_r d(n_i t_i)/dr$]. The fluxes in the parallel direction (along the magnetic field) are taken as classical [11] with flux limits.

The coupling between the transport and turbulence is accomplished through an iterative scheme of the type described in Ref. [9]. The total plasma variable ($= \Psi_k + \psi_k$) is the sum of the slowly evolving, toroidally averaged density and the faster fluctuation density. The characteristic time for the slow toroidal average to change is called τ_0, while the corresponding time for the turbulence is τ_1 ($\tau_1 \ll \tau_0$). For the slow transport density, we solve

$$\frac{\partial \Psi_k^m}{\partial t} + \nabla \cdot (\mathbf{V}_{\parallel i}^m \Psi_k^m + \mathbf{\Gamma_{rk}}^{m-1}) = S_k^m \tag{3}$$

where m is the iteration index. The radial plasma flux from the turbulence simulation is given as

$$\Gamma_{rk}^{m-1} = (1-\alpha_1)\Gamma_{rk}^{m-2} + \alpha_1 \langle \psi_k v_r \rangle^{m-1}, \tag{4}$$

where α_1 is a relaxation parameter in the range [0,1], and the angled brackets denote a double average over the toroidal direction and time for a period τ_1.

The plasma profiles used in the turbulence code to generate the fluxes Γ_{rk}^{m-1} is likewise a relaxed combination of previous profiles, *i.e.*,

$$\Psi_k^{m-1} = (1-\alpha_0)\Psi_k^{m-2} + \alpha_0 \Psi_k^{m-1}. \tag{5}$$

Here α_0 is a second relaxation parameter. Because the 2D transport code is relatively fast, we evolve each plasma transport problem to a steady state, *i.e.*, $\tau_0 \to \infty$.

In the example to follow, we fully couple plasma fluxes from BOUT for the density, and electron and ion temperatures, *i.e.* a particle flux and energy fluxes, thus extending the results given in Ref. [10]. In addition, we also include the convection of the parallel momentum density ($m_i V_\parallel \langle n_i v_r \rangle$) due to the particle flux. We also compute, but do not yet couple, the momemtum flux $m_i \langle v_{\parallel i} v_r \rangle$. Likewise, some energy equation pressure terms are yet to be coupled.

3 Resulting plasma/neutrals profiles and wall fluxes

A coupled simulation is performed the magnetic equilibrium of DIII-D discharge 107404 as shown in Fig. 1. The core boundary ion density and temperatures are fixed to 2.5×10^{19} m^{-3} and $T_e = T_i = 200$ eV, respectively. The plate recycling coefficent is 0.95 and that at the walls is 0.90 to allow for some wall pumping, and to avoid the complication of plasma detachment. Energy transmission boundary conditions are applied at the plates and walls with the electron (ion) loss being $4T_e$ ($2.5T_i$) times the particle flux.

The simulation is initiated by using the plasma density profile generated in Ref. [10] for fixed temperature profiles to obtain fluxes from BOUT, where in addition to the poloidal/radial mesh of 64×50 shown in Fig. 1., 65 points are used for toroidal segment 1/10 the total circumference. These fluxes are used in Eq. 2 to define V_{rk} and D_{rk} for ion density and $T_{e,i}$ in such a way that each contribute equally to the flux. The exception to the 50/50 split is that the minimum diffusion coefficient is set to 0.5 m^2/s for N_i (and 0.25 m^2/s for $T_{e,i}$), and changes in V_{rk} are then adjusted to give the correct total flux. These transport coefficients are transferred to UEDGE to calculate new plasma profiles. For each successive iteration between UEDGE and BOUT, the relation parameters $\alpha_1 = \alpha_0 = 0.5$ in Eqs. 4-5.

The convective component of the plasma fluxes after 7 iterations is shown in Fig. 2 at the outer midplane. Here $\bar{V}_n = \langle n_i v_r \rangle / N_i$ and similarly for $T_{e,i}$. There is a strongly increasing transport outside the separatrix for N_i that is qualitatively consistent with the notion of "blob" propagation [5]. The small negative convection in some regions is typically the result of compensating for the minimum diffusion used of 0.5 m^2/s for N_i and 0.25 for $T_{e,i}$. The convergence of the iteration procedure beyond iteration 7 interrupted by the growth of large t_e fluctuations near the wall where t_e/T_e begins to exceed unity, an unacceptable nonphysical limit. We are developing BOUT modifications to properly simulate regions where t_e/T_e is large. On the other hand, this problem applies to the far SOL region where the transport is already quite large, so the large outward transport there is unlikely to change.

The profiles of densities and temperatures at the outer midplane for iteration 7 are shown in Fig. 3. We also compare with a base-case that uses customary constant diffusion coefficients of 0.33 m^2/s for density, and larger values for pararallel momentum (0.5 m^2/s) and plasma temperatures (1.0), resulting in about 1 MW power input from the core. The differences with strong convection are not so large, except for naturally longer scale lengths in the outer SOL, the T_e core profile, and the much larger neutral density. Of course, differences can be accentuated by using difference constant diffuion values.

Turning to the outer divertor plate, the profiles of particle and heat fluxes are compared in Fig. 4. Here the result with coupling to the turbulence code shows the impact of strong outward convection in the SOL by broaden both the particle and heat fluxes. The broadness of the profiles, especially near the separatrix, may be significantly affected by $\mathbf{E}\times\mathbf{B}$ shear stabilization of the turbulence, which is not included in the present simulations.

The impact of the self-consistent transport is seen most dramatically on the fluxes to the outer wall as shown in Fig. 5. There is both much larger wall flux for the coupled turbulence case, and the fluxes are focused on the outboard region of the SOL, between the upper X-point and the lower X-point as shown in Fig. 1; such "ballooning" character for the turbulence is expected from the unfavorable magnetic curvature on the outside of the torus [1]. While the upper X-point is not included in the simulation domain, its impact is felt through a minimum in the poloidal magnetic field, B_p, in this region. The peak of fluxes near the upper X-point is partially caused by the gradient of the turbulence scaling as $\nabla_2 \sim 1/B_p$, such that the turbulent velocity $v_r = -\nabla_2\phi/B$ can become large there. For the constant diffusion case, the wall fluxes are much less. In terms of global particle and power heat fluxes, the case considered shows that the wall particle and power fluxes are about 40% of those to the divertor plates; these ratios are similar because of the fortuitously similiar wall and plate temperatures.

The corresponding ion and neutral densities along the outer wall are shown in Fig. 6. The neutral density is a direct consequence of recycling from the large ion flux. Over the main chamber region on the outside of the torus, the neutral density is $\sim 10^2$ times that for the constant diffusion case. The peaks near each end are associated with divertor plate recycling.

4 Summary

A method for obtaining a self-consistent model of edge-plasma turbulence and profiles is described. The algorithm couples 2D tranport and 3D turbulence simulations where each code is run on its own characteristic time scale. During each cycle of the iterative procedure, the toroidally averaged plasma profiles are evolved to steady state including particle recycling. A fraction of these profiles are used to update the profiles driving fluctuations in the 3D turbulence code. Likewise, a fractional update of the turbulent fluxes are provided to the transport code from the turbulence simulation. The result is a statistically-averaged steady state.

The procedure is illustrated with a simulation for a DIII-D single-null configuration, and compared with a simple case having constant cross-field diffusion. The self-generated turbulence leads to strong radial transport in the far SOL, as inferred by experimental diagnostics. About 40% of the particle and power flux go to the main chamber wall for this case. While the coupling strategy appears to remain stable, the ultimate iterative convergence of the case considered is restricted by far SOL fluctuations reaching levels of 100%, which requires improvements to the turbulence simulation.

A complementary procedure is to evolve the profiles on each turbulence time step [13]. While costly for times relevant to recycling-induced profile modifications, this method more accurately describes the influence of large, short-time profile adjustments to the turbulence. In the future, we will work to combined this method with longer time-scale procedure described here.

In addition to the power flux to the main chamber wall, an important issue for reactors is the charge-exchange sputtering caused by neutrals penetrating to higher T_i regions of the edge. The possible impact of these charge-exchange neutrals has been estimated for an ARIES-RS configuration in Ref. [8] with the conclusion that wall erosion rates could be much larger than previous estimates.

Acknowledgments

We thank S.I. Krasheninnikov, D.D. Ryutov, and D.G. Whyte for helpful discussions. This work was performed under the auspices of the U.S. Department of Energy by the University of California Lawrence Livermore National Laboratory under contract No. W-7405-Eng-48 and was supported by LLNL LDRD project 03-ERD-009.

References

[1] X.Q. Xu, R.H. Cohen, T.D. Rognlien, and J.R. Myra, Phys. Plasmas **7** (2000) 1951.

[2] T.D. Rognlien, D.D. Ryutov, N. Mattor, and G.D. Porter, Phys. Plasmas **6** (1999) 1851.

[3] B. LaBombard, M.V. Umansky, R.L. Boivin *et al.*, Nucl. Fusion **40** (2000) 2041.

[4] J.A. Boedo, D.L. Rudakov, R.A. Moyer *et al.*, Phys. Plasmas **10** (2003) 1670.

[5] S.I. Krasheninnikov, Phys. Lett. A **283** (2001) 368.

[6] M.V. Umansky, S.I. Krasheninnikov, B. LaBombard *et al.*, Phys. Plasmas **6** (1999) 2793.

[7] A.Yu. Pigarov, S.I. Krasheninnikov, T.D. Rognlien *et al.*, Contrib. Plasma Phys. **44** (2004) 228.

[8] M. Kotschenreuter, T.D. Rognlien, and P. Valanju, subm. to Fusion Eng. Design (2004).

[9] A.I. Shestakov, R.H. Cohen, J.A. Crotinger, L.L. LoDestro, A. Tarditi, and X.Q. Xu, J. Comp. Phys. **185** (2003) 399.

[10] T.D. Rognlien, M.V. Umansky, X.Q. Xu, and R.H. Cohen, Contrib. Plasma Phys. **44** (2004) 188.

[11] S.I. Braginskii, Transport processes in a plasma, *Reviews of Plasma Physics*, Vol. 1, Ed. M.A. Leontovich (Consultants Bureau, New York, 1965), p. 205.

[12] M.V. Umansky, T.D. Rognlien, and X.Q. Xu, this conf., paper 303.

[13] X.Q. Xu, W.M. Nevins, R.H. Cohen *et al.*, Contrib. Plasma Phys. **44** (2004) 105.

Figure captions

(1) Poloidal/radial simluation domain and mesh (64×50) for BOUT/UEDGE coupled simulation of DIII-D discharge 107404.

(2) Effective convective velocities at the outer midplane for density and temperatures from BOUT after 7 iterations.

(3) Outer midplane profiles of (a) ion and neutral densities, and (b) temperatures at from UEDGE after 7 iterations. The dashed lines show results for N_i and T_e with constant diffusion.

(4) Outer divertor plate profiles of (a) ion particle flux, and (b) heat flux comparing results with 7 iterative BOUT/UEDGE coupling and the initial case with constant diffusion coefficients.

(5) Outer wall profiles of (a) ion particle flux, and (b) heat flux comparing results with 7 iterative BOUT/UEDGE coupling and with constant diffusion coefficients.

(6) Outer wall profiles of ion and neutral density comparing results with 7 iterative BOUT/UEDGE coupling and with constant diffusion coefficients.

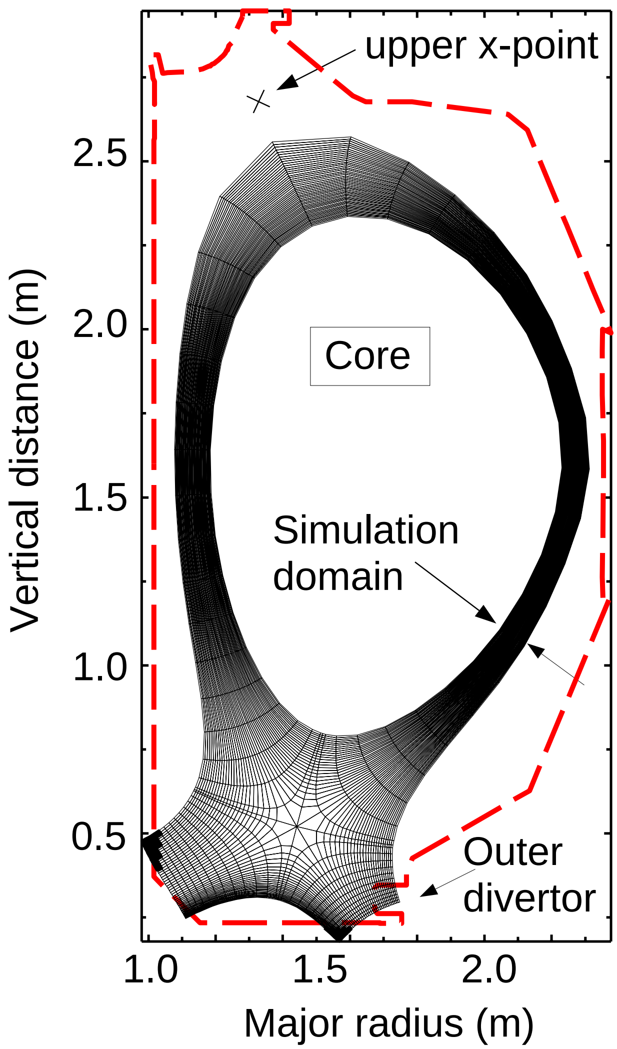
upper x-point
Core
Simulation
domain
Outer
divertor
Vertical distance (m)
2.5
2.0
1.5
1.0
0.5
1.0
1.5
2.0
Major radius (m)

Fig. 1

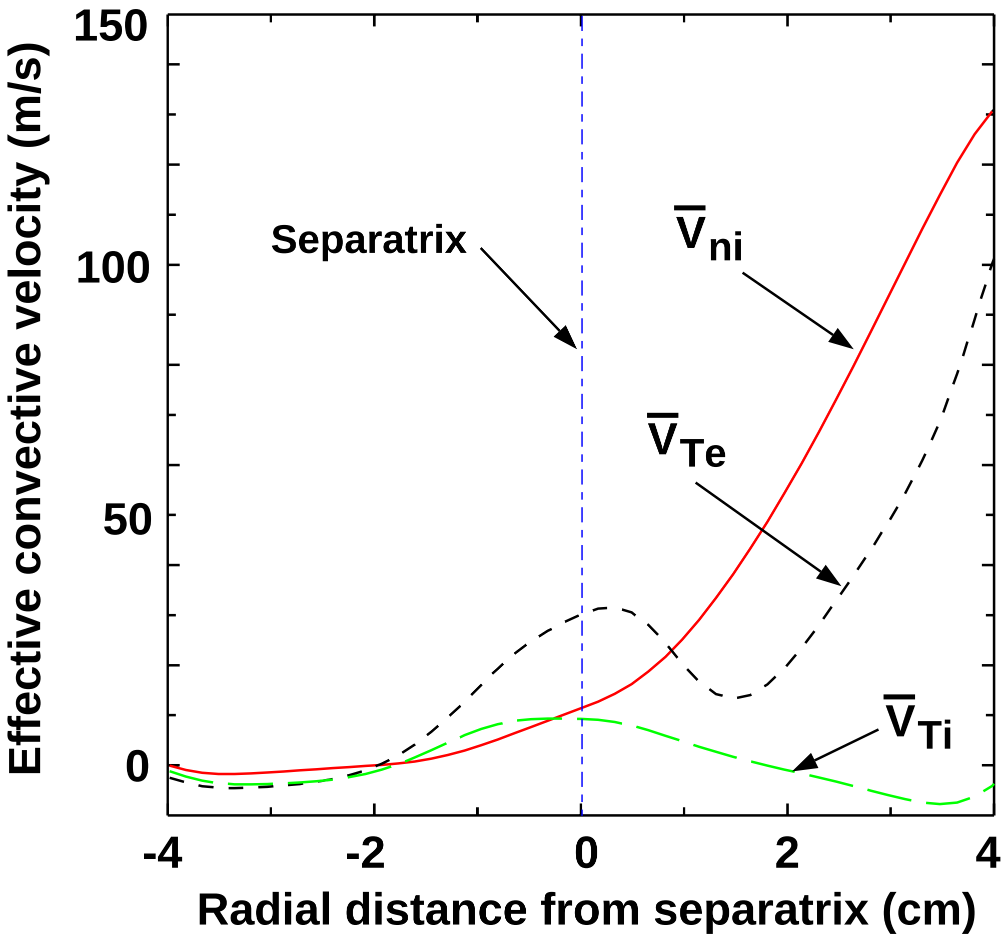

150
100
50
0
Effective convective velocity (m/s)
Separatrix
$\overline{V}_{ni}$
$\overline{V}_{Te}$
$\overline{V}_{Ti}$
-4
-2
0
2
4
Radial distance from separatrix (cm)

Fig. 2

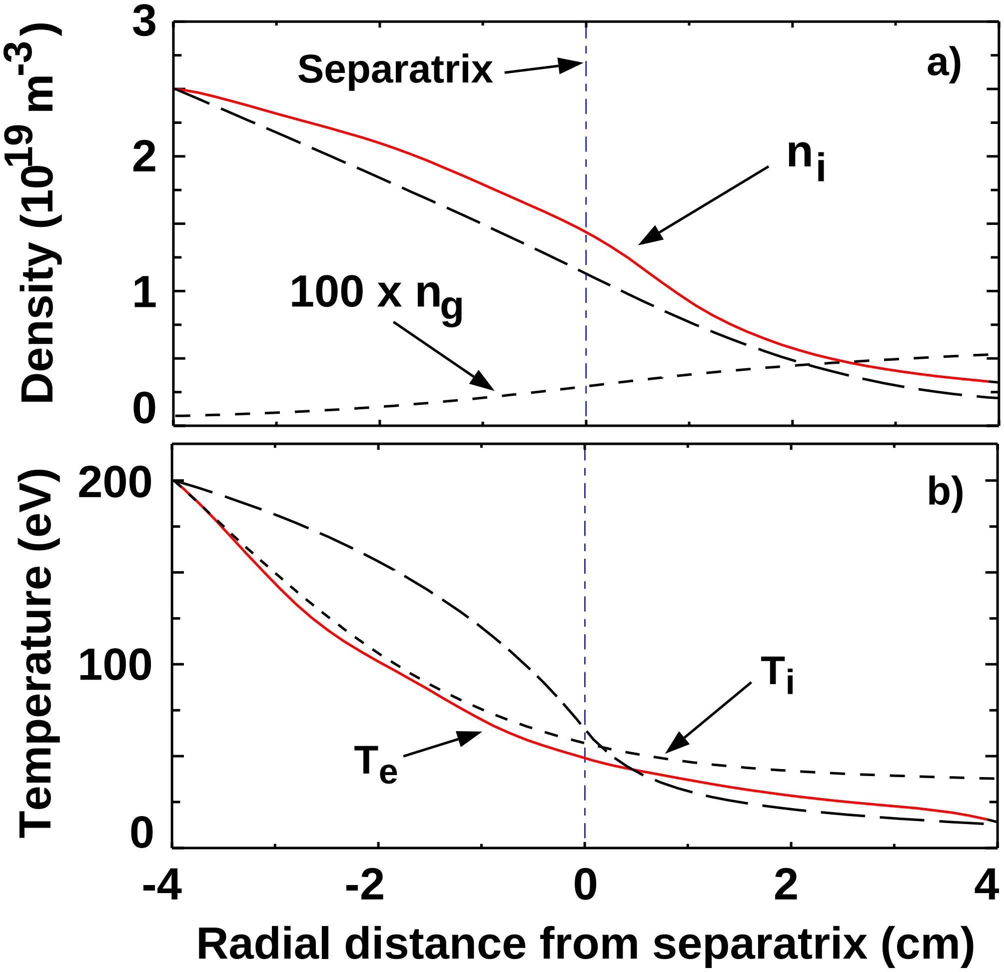
3
2
1
0
Density (10^{19} m^{-3})
Separatrix
a)
n_i
100 x n_g
200
100
0
Temperature (eV)
b)
T_i
T_e
-4
-2
0
2
4
Radial distance from separatrix (cm)

Fig. 3

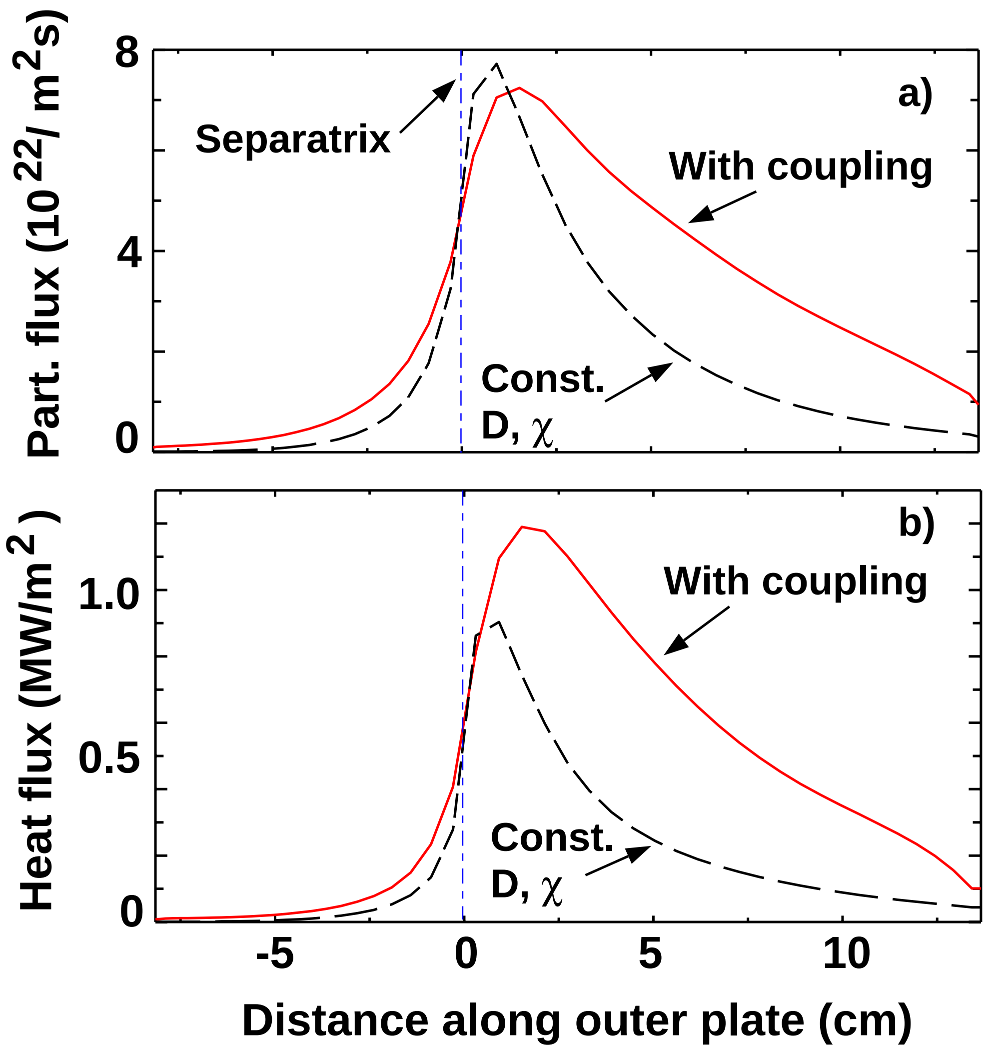

Part. flux (10^{22}/ m^2s)
8
4
0
a)
Separatrix
With coupling
Const.
D, χ
Heat flux (MW/m^2)
1.0
0.5
0
b)
With coupling
Const.
D, χ
-5
0
5
10
Distance along outer plate (cm)

Fig. 4

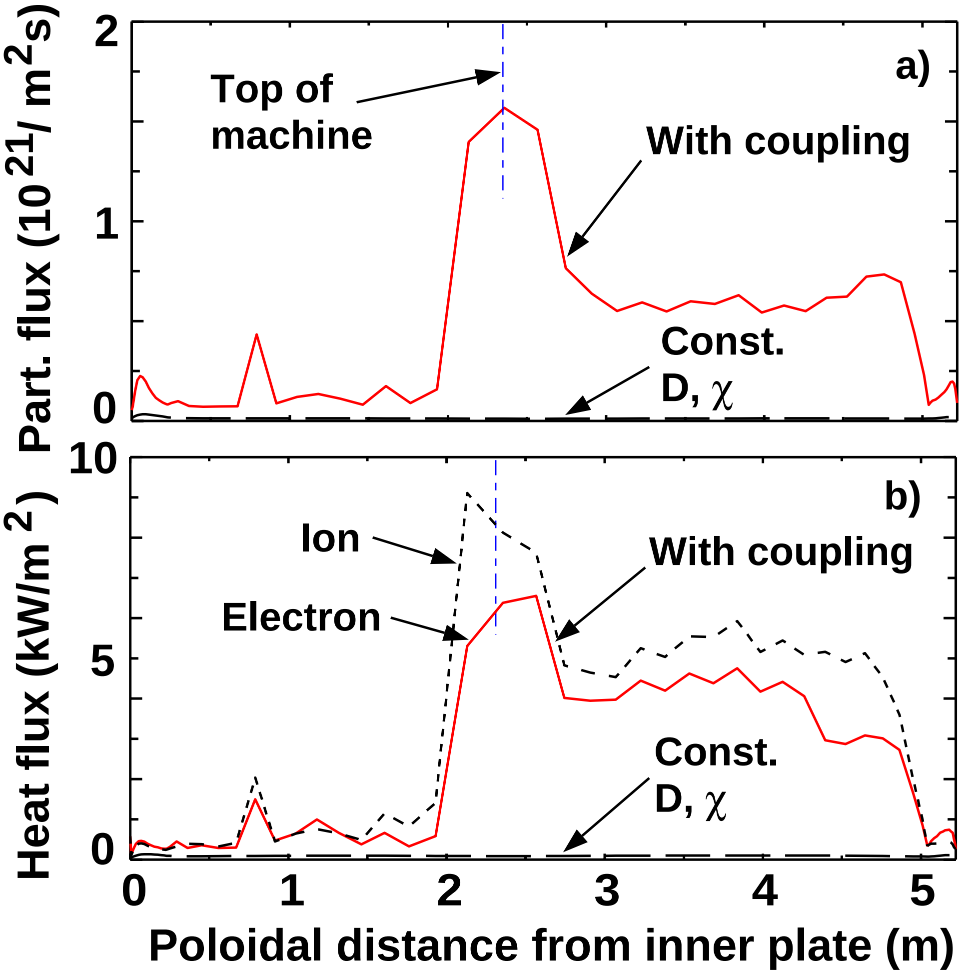

2
1
0
10
5
0
Part. flux (10^{21}/ m^2s)
Heat flux (kW/m^2)
a)
Top of machine
With coupling
Const. D, χ
b)
Ion
Electron
With coupling
Const. D, χ
0
1
2
3
4
5
Poloidal distance from inner plate (m)

Fig. 5

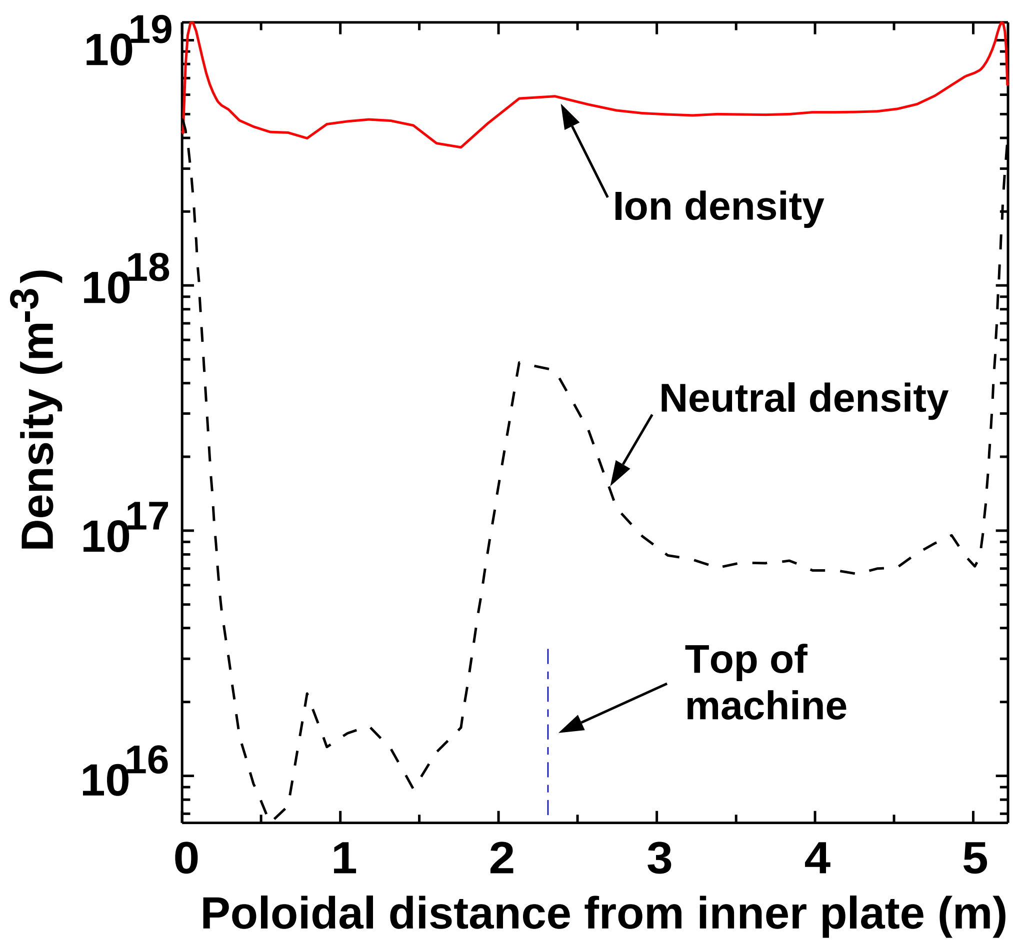

10^{19}
10^{18}
10^{17}
10^{16}
Density (m^{-3})
Ion density
Neutral density
Top of machine
0
1
2
3
4
5
Poloidal distance from inner plate (m)

Fig. 6